COBEM 2023 27TH INTERNATIONAL CONGRESS OF MECHANICAL ENGENEERING

ABCM Brazilian Society of Mechanical Sciences and Engineering
27th ABCM International Congress of Mechanical Engineering
December 04-08, 2023, Florianópolis-SC, Brazil

COB-2023-2406
SYNTHESIS AND CHARACTERIZATION OF THE HIGH-ENTROPY ALLOY CrMnFeCoNi OBTAINED BY MECHANICAL ALLOYING

Felipe Martina André
Claudio Michel Poffo
Daniel Cunha
Athos Fernandes Araújo
Catarina Meiko Hayashi
Programa de Pós-Graduação em Ciência e Engenharia de Materiais - Universidade Federal de Santa Catarina - Campus Universitário – Bloco A do Depto. de EMC C.x. Postal 476 CEP.: 88.040-900 – Florianópolis
felipe.martina@posgrad.ufsc.br
claudio.poffo@ufsc.br
daniel.cunha@ufsc.br
athos.araujo@posgrad.ufsc.br
hayashi.h@posgrad.ufsc.br

Abstract. *High entropy alloys are a class of metallic materials composed at least 5 different elements in concentrations ranging from 5-35%. This paper sought to synthesize a high entropy alloy composed of Chromium, Manganese, Iron, Cobalt and Nickel in equiatomic proportions, through high energy mechanical milling (Mechanical Alloying) and to characterize its physical and chemical properties. The alloy was submitted to X-ray diffraction (XRD) to evaluate the structural evolution, after 5 hours of milling the material presented FCC and BCC structure. After 10 hours of milling, the same structures were maintained, but with a higher concentration of defects in its structure, evidencing the high structural stability for the high entropy alloy. The crystallite size was calculated using the Scherrer equation. It was observed that after 5 hours of grinding, the crystallites reached a size of 7.2 nm for the FCC phase and 7.7 nm for the BCC phase. After 10 hours of grinding, the values for the FCC and BCC phases changed to 7.8 nm and 5.9 nm, respectively. Photoacoustic Absorption Spectroscopy (PAS) tests were performed to calculate the thermal diffusivity of the material, the results showed a tendency to reduce thermal diffusivity with increasing milling time.*

Keywords: *High entropy, grinding, crystallinity, thermal diffusivity.*

1. INTRODUCTION

The study and development of new materials are closely related to the evolution and technological progress of civilization. Most metallic alloys widely used in the industry for commercial purposes were developed in the 1970s, where one element was used in large concentrations, and other elements were added in small quantities to obtain variations in their physical properties. The classic example of this is the production of steel, where additions of small amounts of alloying elements can significantly alter its mechanical properties. Through this process, it is possible to obtain alloys with good properties and many applications. However, it is common to need to improve the properties of the alloy by adding elements with high concentrations and eventually manufacturing alloys with equiatomic concentrations. (Bobbili, R.; Madhu, V. 2018)

Between 2003 and 2004, two independent research studies by S. Ranganathan and Jien-Wei Yeh, respectively, initiated a new line of research in alloys composed of multiple elements in equiatomic proportions. These alloys were named High-Entropy Alloys (HEAs) and showed promising results, particularly in terms of mechanical properties. Based on the findings of these studies, new researchers embraced the study of this new class of metallic materials, leading to a rapid increase in the number of publications. (Ranganathan, S. 2003)

This new class of metallic alloys aims to enhance properties that common metallic alloys are unable to meet. The objective is to obtain an alloy composed of a minimum of 5 different elements in atomic proportions ranging from 5-35%, and which exhibit configurational entropy greater than 12.4 J/mol.K.

Due to their unique characteristics, high-entropy alloys have the potential to yield materials with excellent mechanical properties, offering a wide range of possible applications. These alloys exhibit high performance at elevated temperatures, excellent ductility and fracture toughness, superparamagnetism, superconductivity, high strength at cryogenic temperatures, and high oxidation resistance. (Alaneme, K.; Bodunri, M.; Oke, S. 2016)

This work aimed to synthesize a high-entropy alloy composed of CrMnFeCoNi and characterize its structure and thermal properties (thermal diffusivity). The alloy was prepared to achieve an equiatomic composition, and the material was processed using the mechanical milling method with a Ball to Powder Ratio (BPR) of 7:1.

2. IMPORTANT CONCEPTS

2.1 High entropy alloys

High entropy alloys (HEA) are defined based on the complexity of their composition. These alloys have a minimum of five distinct elements, with compositions ranging from 5 to 35%. However, a HEA cannot be defined solely based on the number of elements it contains. For an alloy to be considered an HEA, it must exhibit a single phase in solid solution. In some cases, high-entropy alloys may exhibit two phases. (Zhang et al, 2016; Otto et al, 2013)

The alloys are considered to have low entropy when they exhibit ΔS_{conf} less than 0.69R, medium entropy between 0.69R and 1.61R, and high entropy when ΔS_{conf} is greater than 1.61R, where R is the gas constant. To obtain the configuration entropy, the following relation is used: $\Delta S_{conf} = -R\sum XilnXi$, where Xi represents the molar fraction of each constituent element in the chemical composition of the alloy. (Miracle et al, 2014)

HAE exhibit four characteristic effects, namely: the effect of crystal lattice distortion, due to the different elements that constitute an HEA and its equiatomic composition. The crystal lattice formed in a solid solution undergoes deformation caused by the difference in atomic radii between the elements (figure 1). This effect is due to the high configurational entropy of the alloy, which promotes the formation of a solid solution between the components, preventing the formation of intermetallic compounds and leading to a simple crystalline structure in HEA. (Zhang et al, 2016, Cantor, 2004)

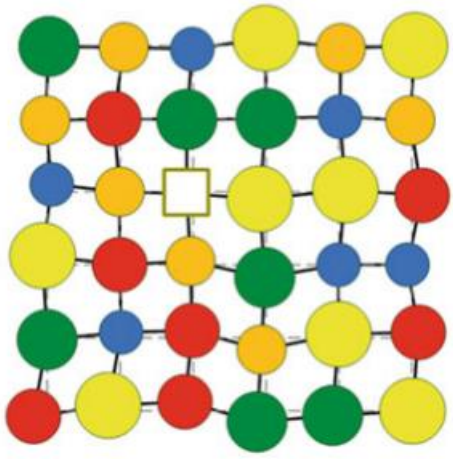

Figure 1. Severe lattice distortion caused by the difference in atomic radius (Zhang et al. 2016)

The slow diffusion effect is directly related to the slow atomic diffusion kinetics found in HEA, which is caused by the distortion in their crystal lattice. The lattice distortion limits atomic movement, reducing the diffusivity of the alloy. (Pickering, E. Jones, N, 2016)

The cocktail effect refers to the fact that the mechanical properties of HAE are not solely based on the characteristics of the individual elements that constitute them, as predicted by the rule of mixtures. The alloy is influenced by the mutual interactions among its constituent elements, such as severe lattice distortion. (Zhang et al, 2016)

2.2 Mathematical equations

The crystallite size of the material was calculated using the Scherrer equation, which relates the radiation used in X-ray diffraction (λ), the width of the diffraction peak at half maximum intensity (β) known as FWHM, and the diffraction angle (θ). The equation 1 is presented as follows:

$$d = \frac{0{,}91\lambda}{\beta \cos(2\theta)}, \quad (1)$$

The thermal diffusivity of the material (α) is obtained through equation 2, which relates the sample thickness (L, table 1) to the slope of the linearized graph of frequency vs. signal and frequency vs. phase (a). The equation 2 is presented as follows:

$$\alpha = \pi \left(\frac{L}{a}\right)^2, \quad (2)$$

3. MATERIALS AND METHODS

The precursor powders used in this work were elements with a high degree of purity: Fe (99.5%), Cr (99.8%), Mn (99.3%), Co (99.8%), and Ni (99.9%). The elements were prepared to obtain an equiatomic alloy for the formation of the high-entropy alloy CrMnFeCoNi. The Ball-to-Powder Ratio (BPR) used was 7:1, indicating the ratio of the masses of the milling balls to the precursor powders.

After preparing the equiatomic mixture of elements, the mechanical milling process was initiated using the high-energy vibratory mechanical mill, specifically the SPEX 8000M model. The material was sealed in a stainless-steel cylinder and closed under an argon atmosphere to prevent contamination from atmospheric air.

Initially, the material was mixed in the mill for 5 minutes without the presence of grinding media to ensure that the precursor powders were well mixed before starting the milling process. After the 5-minute mixing step, the grinding jar was opened, and grinding media weighing a total of 43.9407 g were added. The mass of the material being milled was 6.2746 g.

The milling process was halted at hourly intervals to collect material samples intended for thermal diffusivity measurement analyses. Samples were obtained after 1, 2, 3, 5, and 10 hours of milling. The sample preparation procedure involved powder compaction using a hydraulic press under a load of 8000 kgf, yielding pellets with a consistent 10 mm diameter, while their thicknesses and masses varied, as delineated in Table 1.

Table 1. Thickness of each sample corresponding to the milling period.

Time (h)	**1**	**2**	**3**	**5**	**10**
Thickness (μm)	481	526	559	482	403
Mass (g)	0,301	0,331	0,351	0,303	0,253

The PAS equipment, which measures the thermal conductivity of the material. It consists of a light source that emits light onto the material. This light initially passes through a water barrier, which filters out the infrared radiation from the light. After that, the light is frequency-modulated by a chopper, which controls how many times per second the light hits the sample's surface. The light is then focused on the sample through lenses and finally reaches the sample itself.

After 5 hours of milling, the material was removed to perform an X-ray diffraction (XRD) test to evaluate if the expected crystalline phase had formed. A Rigaku MiniFlex600 X-ray diffractometer was employed, utilizing copper radiation (λ=0.154 nm), over an angular scanning range of 20-100° with a scanning rate of 10°/min. After the XRD test was conducted on the 5-hour milled sample, the material was milled for an additional 5 consecutive hours, totaling 10 hours of the milling process. The crystallite sizes were calculated using the width of the X-ray diffraction peaks, which relates the radiation used in X-ray diffraction, the width of the diffraction peak at half maximum intensity, and the diffraction angle.

4. RESULTS AND DISCUSSIONS

4.1 Structural characterization

After 5 hours of high-energy mechanical milling, the material was subjected to X-ray diffraction (XRD) analysis to evaluate the formation of a high-entropy phase for the CrMnFeCoNi alloy. The diffraction pattern is shown in Figure 2.

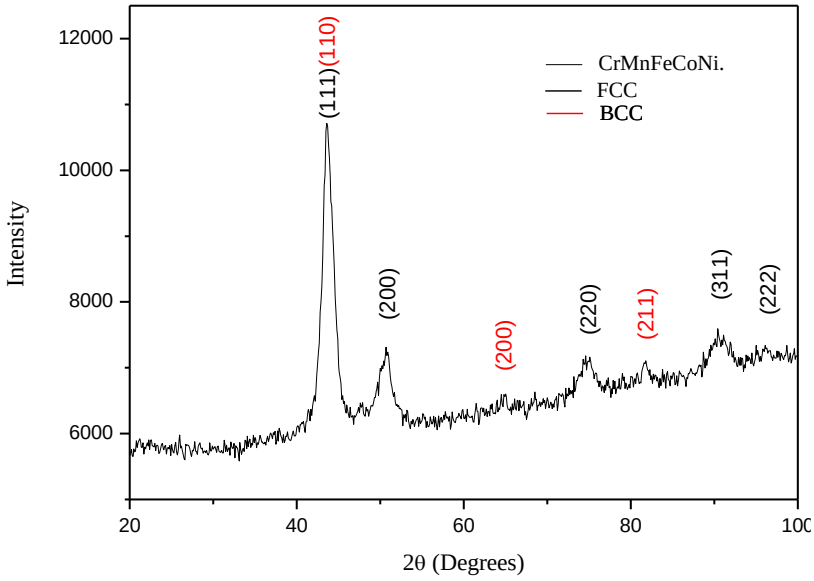

Figure 2. XRD analysis for the material subjected to 5 hours of milling.

Based on Figure 2, it is possible to observe well-defined diffraction peaks, indicating the formation of crystalline phases of both face-centered cubic (FCC) and body-centered cubic (BCC) structures. This result can be compared to the work conducted by Ni *et al* (2019), where they obtained the same crystalline structure for the same alloy with the same chemical composition and Yu *et al* (2016).

The first diffraction peak, around 44°, represents the sum of the peaks from the two distinct phases. Therefore, a Lorentz curve was plotted to determine the individual peaks corresponding to each phase present in the structure. The result is shown in Figure 3.

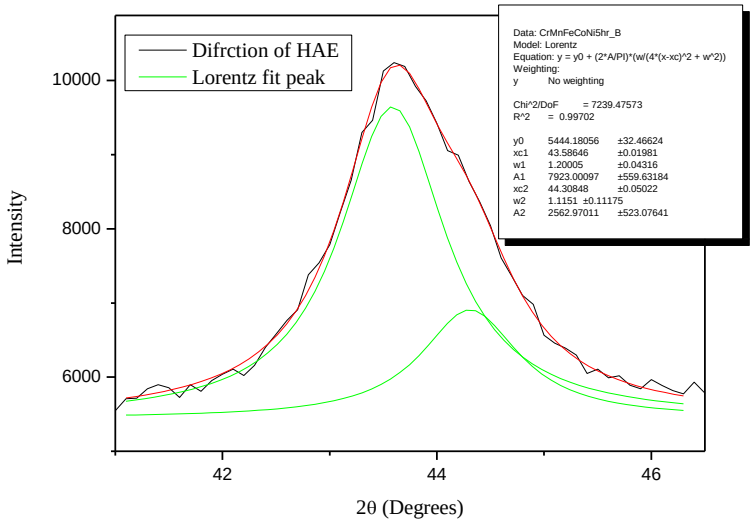

Figure 3. Lorentzian curves for the first diffraction peak after 5 hours of griding.

The crystal size for the formed phases was calculated using Equation 1 based on the first diffraction peak. The values used for the calculation are presented in Figure 6. The radiation used was copper (λ=0.15406 nm), and the FWHM should be in radians. In 5 hours of milling, the FCC phase has a crystal size of 7.2 nm, while the BCC phase has a crystal size of 7.7 nm.

The alloy was subjected to the grinding process for an additional 5 hours, totaling 10 hours of grinding. The objective was to analyze the structural stability of the alloy and how it behaves when subjected to a longer grinding period. The result for the material ground for 10 hours is presented in Figure 4.

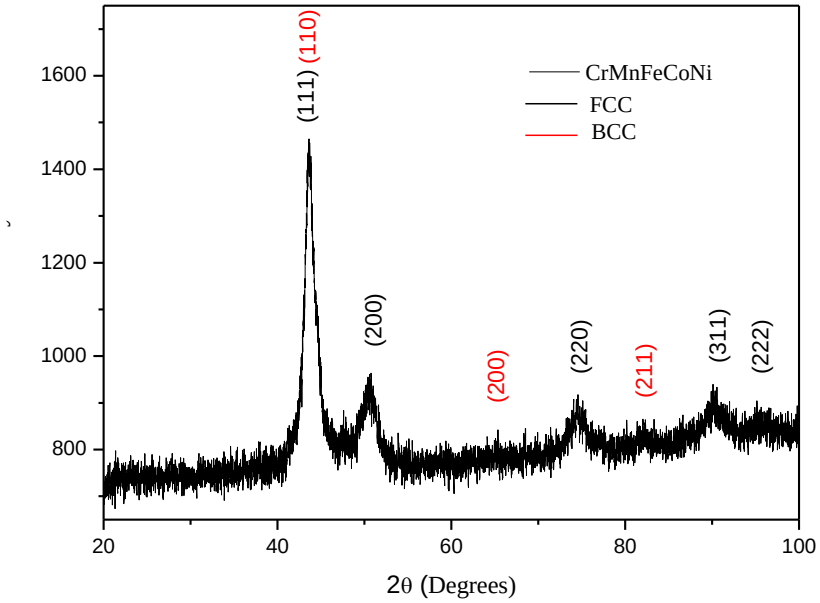

Figure 4. XRD analysis for the material subjected to 10 hours of milling.

It is observed that after 10 hours of mechanical grinding, the alloy still exhibits the same crystalline phases. This is evident as the diffraction peaks are still at the same positions for 2θ, indicating that the alloy has high structural stability. To assess the influence of the additional 5 hours on the high-entropy alloy, the diffraction pattern was plotted for the material with 5 and 10 hours of grinding. The result is presented in Figure 5.

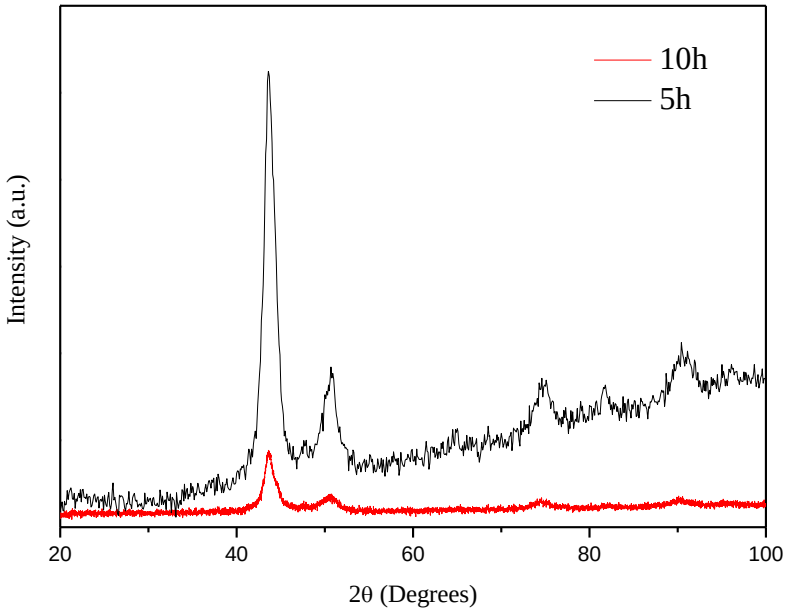

Figure 5. Comparison of the XRD pattern for 5 and 10 hours of grinding.

Based on Figure 8, it is possible to perceive that the diffraction peaks remain in the same regions, but with significantly reduced peak intensities for the 10-hour grinding pattern. This reduction in intensity is possibly caused by the accumulation of crystalline defects generated in the material due to the prolonged exposure to high-energy mechanical grinding. As the number of defects in the material's structure increases, such as dislocations, vacancies, and grain boundaries, the intensity of the diffraction peaks decreases. These defects act to decrease the reflection of X-rays incident on the material.

The same method used previously was adopted to calculate the crystallite size for both phases in the material ground for 10 hours. The diffraction peak is shown in Figure 6.

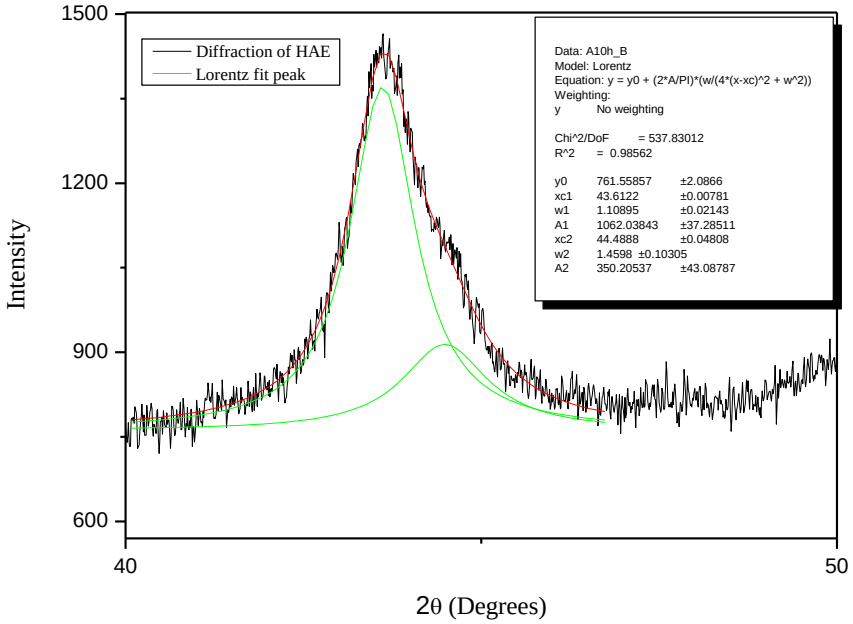

Figure 6. Lorentzian curves for the first diffraction peak after 10 hours of griding.

The crystallite sizes for the FCC phase after 10 hours of grinding are 7.8 nm, while the CCC phase showed crystallites of 5.9 nm. We can observe that for the FCC phase, the crystallite size had a small increase, while the CCC phase experienced a reduction. The observed decrease in the proportion of the CCC phase can be attributed to its metastable nature. This is because the CCC phase is not represented in the phase diagram that correlates the crystal structure of a material with the electron concentration in the valence electron layer (VEC). It is observed that for alloys with VEC values ≥ 8, the crystal structure of the high-entropy alloy tends to predominantly crystallize in the FCC phase. When VEC is within the range of 6.87 to 8, it is common for alloys to exhibit a coexistence of the FCC and BCC phases. On the other hand, the increase in the proportion of the FCC phase can be explained by the transformation of the CCC phase into FCC, which is thermodynamically more stable. This reflects the intrinsic tendency of the alloy to predominantly crystallize in the FCC phase, as predicted by the thermodynamic parameters that govern the formation of crystal phases. Zhang et al, 2016)

4.2 Thermal characterization

Based on the data provided in the PAS (Photoacoustic Absorption Spectroscopy) assay, including frequency "f" (Hz), signal "s" (mW), and signal phase "Φ" (radians), these values are used to linearize the graph for data processing. In the initial regime, specifically at low frequencies of light modulation, the mechanism of non-radiative intra-band thermalization is observed. For data processing, the square root of frequency ($\sqrt{f}$) versus natural logarithm of the signal (ln(s)) and square root of frequency ($\sqrt{f}$) versus signal phase (Φ) in radians are used. By analyzing these curves, the region where the angular coefficient is the same for both curves is identified, as this is where the mechanism of interest occurs. Using the value of the angular coefficient, Equation 2 is applied to determine the thermal diffusivity of the material.

The following Figure 7 shows the results for the sample ground for 1 hour, focusing on the region where the curves exhibit the same angular coefficient. The X-axis of the Figures represents frequency, while the left Y-axis represents the photoacoustic signal in arbitrary units, and the right Y-axis represents the phase of the photoacoustic signal, also in arbitrary units.

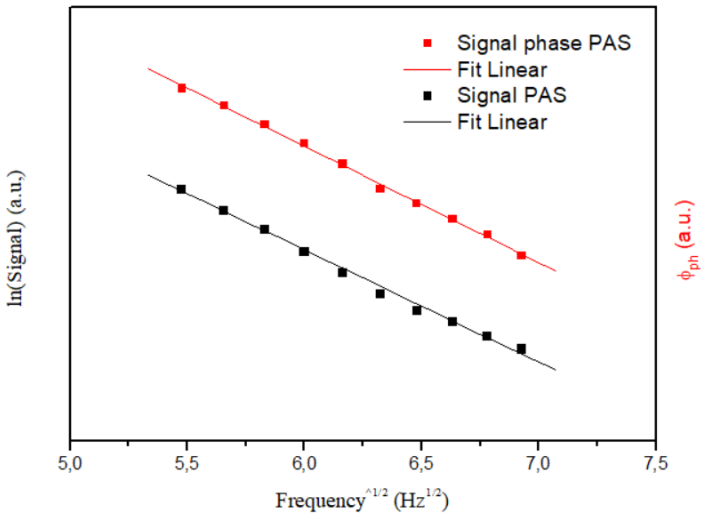

Figure 7. Amplitude and phase of the photoacoustic signal for a 1-hour ground sample.

For better visualization, the results of angular coefficients are presented in table 2, where by taking the thickness values of the samples shown in table 1 and applying equation 2, we obtain the thermal diffusivity of the material. Also presented in table 2.

Table 2. angular coefficient of the linearized graph and thermal diffusivity of the alloy.

Milling (h)	**1**	**2**	**3**	**5**	**10**
Angular coefficient	-0,26329	-0,30399	-0,33603	-0,31671	-0,34601
Thermal Diffusivity (cm^2/s)	0,1048	0,09406	0,08694	0,07276	0,04507

Assuming the values obtained experimentally, the following diffusivity profile over the material milling time is shown in Figure 8. Based on the results presented in Table 2, it can be observed that the thermal diffusivity of the alloy decreases as the milling time increases. These results are expected because the effect of diffusivity is related to the movement of phonons in the material's structure. As the material is milled for a longer time, it gradually forms a crystalline phase in solid solution, which exhibits grain boundaries that act as barriers hindering the movement of phonons. Consequently, the thermal diffusivity of the alloy decreases. Additionally, the distortion of the crystal lattice also contributes to this reduction in diffusivity, as shown. (Senkov, 2011)

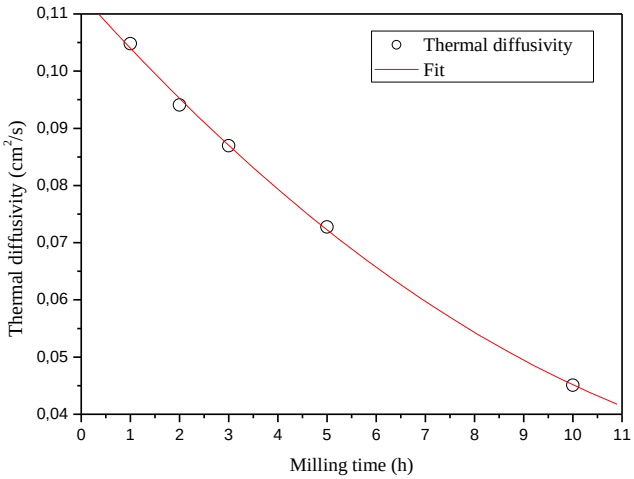

Figure 8. Diffusivity profile as a function of milling time for the high entropy alloy.

After 5 hours of milling, when the material forms the crystalline phase, the diffusivity significantly decreases, as shown in the 5-hour sample measurement. This phenomenon is related to the large number of crystalline defects that are

introduced into the material due to the prolonged milling period. These defects include vacancies, dislocations, and grain boundaries.

The effect of increased defects in the material can be observed in Figure 8, where X-ray diffraction (XRD) analysis shows that the material still retains the same crystalline structures but with a higher concentration of defects in its structure. This is characterized by lower intensity and broader peaks in the diffraction pattern.

5. CONCLUSIONS

In this study, a high entropy alloy composed of CrMnFeCoNi in equiatomic proportions was synthesized using mechanical alloying in a vibratory mill. The material was characterized through X-ray diffraction (XRD) tests to analyze the crystalline structure and crystallite size, as well as photoacoustic absorption spectroscopy (PAS) to obtain the thermal diffusivity of the alloy. These characteristics were analyzed as a function of the material's milling time. It was observed that after 5 hours of milling, the alloy crystallizes into a majority face centered cubic (FCC) phase and a minority body centered cubic (BCC) phase, forming a high-entropy alloy. After 10 hours of milling, the alloy maintains the same high entropy phases but with an increased number of defects in its structure due to the high-energy mechanical milling synthesis technique, resulting in reduced diffraction peak intensities. The material milled for 5 hours exhibited crystallites with dimensions of 7.2 nm (FCC) and 7.7 nm (BCC). However, after 10 hours of milling, these values changed to 7.8 nm and 5.9 nm for FCC and BCC, respectively, indicating a tendency for the alloy to crystallize into an FCC structure. The thermal diffusivity of the alloy decreases as the milling time increases, attributed to the formation of the high-entropy alloy with its distorted structure, which hinders phonon movement, and the accumulation of defects in the material's crystalline structure, such as dislocations and vacancies. The thermal diffusivity results indicate that the alloy exhibits low diffusivity compared to most pure metallic materials.

6. ACKNOWLEDGEMENTS

The work presented here was conducted at the Universidade Federal de Santa Catarina. We also thank the members of GESMat, for all their support. This study was also financed by the Coordenação de Aperfeiçoamento de Pessoal de Nível Superior (CAPES).

7. REFERENCES

Alaneme, K. K.; Bodunri, M. O.; Oke, S. R. *Processing, alloy composition and phase transition effect on the mechanical and corrosion properties of high entropy alloys*. Journal of Materials Research and Technology, 384–393, 2016.

Bobbili, R.; Madhu, V. *A Modified Johnson-Cook Model for FeCoNiCr high entropy alloy over a wide*. Materials Letters, 218, 103-105, 2018.

Cantor, B. *Microstructural development in equiatomic multicomponent alloys, Materials Science and Engineering A-Structural materials properties microstructure and processing*. 375-377 (2004) 213-218. [S.l.], 2005.

Campos, Carlos Eduardo Maduro. *Study Of Physical Properties Of Nanomaterials Produced By Mechanical Synthesis*. 2005. 192 p. Thesis (Ph.D.) - Federal University of Santa Catarina.

Koch, C.. *Intermetallic matrix composites prepared by mechanical alloying*, a 70 review. Materials Science and Engineering A, 39-48, 1998.

Miracle, D.; Miller, J.; Senkov, O.; Woodward, C.; Uchic, M. *Exploration and Development of High Entropy Alloys for Structural Applications*. Entropy, 16, 494- 525, 2014.

Ni, X. et al. *Microstructure and properties of CrMnFeCoNi High Entropy Alloy prepared by mechanical alloying and spark-plasma sintering*. Powder Metalurgy, v. 62, n. 1, p. 38-43, 2019.

Otto, F; A. Dlouhý, C. Somsen, H. Bei, G. Eggeler, E.P. George, *The influences of temperature and microstructure on the tensile properties of a CoCrFeMnNi highentropy alloy*, Acta Materialia 61(15) (2013) 5743-5755.

Pickering, E.J. N.G. Jones, *High-entropy alloys: a critical assessment of their founding principles and future prospects,* International Materials Reviews 61(3) (2016) 183-202.

Ranganathan, S. *Alloyed pleasures: multimetallic cocktails*. Curr Sci 85:1404–1406. 2003

Senkov, O.N, G.B. Wilks, J.M. Scott, D.B. Miracle, *Mechanical properties of $Nb_{25}Mo_{25}Ta_{25}W_{25}$ and $V_{20}Nb_{20}Mo_{20}Ta_{20}W_{20}$ refractory high entropy alloys*, Intermetallics 19(5) (2011) 698-706.

Suryanarayana, C. *Mechanical alloying and milling*. Progress in Materials Science, 1-184, 2001.

YU, P. F. et al. The high-entropy alloys with high hardness and soft magnetic property prepared by mechanical alloying and high-pressure sintering. **Intermetallics**, v. 70, p. 82–87, 2016.

Zhang, Y. et al. *High-Entropy Alloys Fundamentals and Applications*. 524p. Springer, 2016.

8. RESPONSIBILITY NOTICE

The authors are the only responsible for the printed material included in this paper.